

See discussions, stats, and author profiles for this publication at: <https://www.researchgate.net/publication/235515821>

# Prediction of high-frequency intrinsic localized modes in Ni and Nb

Article in *Physical review. B, Condensed matter* · October 2011

DOI: 10.1103/PhysRevB.84.144303

CITATIONS

51

READS

85

5 authors, including:



Vladimir Hizhnyakov

University of Tartu

245 PUBLICATIONS 2,422 CITATIONS

SEE PROFILE



Mihhail Klopov

Tallinn University of Technology

40 PUBLICATIONS 243 CITATIONS

SEE PROFILE



Albert John Sievers

Cornell University

463 PUBLICATIONS 10,029 CITATIONS

SEE PROFILE

Some of the authors of this publication are also working on these related projects:



Single shot diagnostic of short electron bunches using coherent radiation. [View project](#)



Spectral hole burning [View project](#)

# Prediction of high frequency intrinsic localized modes in Ni and Nb

M. Haas<sup>1</sup>, V. Hizhnyakov<sup>1</sup>, A. Shelkan,<sup>1</sup> M. Klopov,<sup>2</sup> and A. J. Sievers<sup>3</sup>

<sup>1</sup>*Institute of Physics, University of Tartu, Riia 142, 51014 Tartu, Estonia*

<sup>2</sup>*Institute of Physics, Tallinn University of Technology, Ehitajate 5, 19086 Tallinn, Estonia*

<sup>3</sup>*Laboratory of Atomic and Solid State Physics, Cornell University, USA*

(Dated: December 16, 2013)

It is found that in some metals an intrinsic localized mode may exist with frequency above the top of the phonon spectrum. The necessary condition, requiring sufficiently high ratio of quartic to cubic anharmonicity may be fulfilled because of screening of the interaction between ions by free electrons. Starting from the known literature values of the pair potentials we have found that in Ni and Nb the derived localized mode condition is fulfilled. MD simulations of the nonlinear dynamics of Ni and Nb confirmed that high frequency ILMs may exist in these metals.

PACS numbers: 63.20.Pw, 63.20.Ry, 05.45.-a, 05.45.Yv

## I. INTRODUCTION

The study of vibrational energy localization in highly excited small molecules is well known and a number of reviews have appeared [1-4]. The idea of localization in perfect anharmonic lattices was considered by Kosevich and Kovalev [5] for the case of a monatomic chain with nearest neighbor harmonic, cubic and quartic anharmonic interactions. They showed that an envelop soliton-like excitation with frequency above the top of the phonon band could exist for sufficiently weak cubic interactions. Somewhat later strongly localized vibrational modes in anharmonic lattices were proposed in Refs. [6,7]. The realization that this new excitation phenomenon only required nonlinearity plus discreteness expanded the topic in different directions, ranging from analytical considerations [6-9] to MD simulations [10-12]. The early reviews of the resulting field focused on predicting different processes [13-15]. These excitations, which are often referred to as intrinsic localized modes (ILMs), discrete breathers or discrete solitons, have now been identified in different driven physical systems including electronic and magnetic solids, Josephson junctions, micromechanical arrays, optical waveguide arrays, and laser-induced photonic crystals [16-18].

In numerical studies of ILMs in atomic lattices different two-body potential models such as Lenard-Jones, Born-Mayer-Coulomb, Toda, and Morse potentials as well as their combinations have been used in the past. All of these potentials show strong softening with increasing vibrational amplitude and the ILMs, found in these simulations, always drop down from the optical band(s) into the phonon gap, if there is one. (See Refs. [19-22], where ILMs in alkali halide crystals have been calculated). Consequently, it has been assumed that the softening of atomic bonds with increasing vibrational amplitude is a general property of crystals and therefore ILMs with frequencies above the top phonon frequency cannot occur. However recent inelastic neutron scattering investigation of the vibrational excitations in uranium ( $\alpha$ -U) in thermal equilibrium showed some degree of localiza-

tion near the top of the phonon spectrum at elevated temperatures [23]. For this to occur the pair potentials in this metal must be fundamentally different from those describing alkali halide crystals. Because the electrons at the Fermi surface provide an essential contribution to the screening of the ion-ion interaction in metals there is no apriori reason to expect the anharmonicities of these two very different systems to be similar.

The purpose of this paper is to explore the ILM properties in nickel and niobium by starting from the embedded atom model (EAM). This technique allows one to find the potential energy of vibrations in metals, taking the screening effects into account [24,25]. Our findings show that ILMs may be expected to occur in both of these metallic crystals. In the next section we illustrate how the elastic springs of the atomic bonds are to be renormalized to give the minimal condition for localized mode production. In the small ILM amplitude limit two additive contributions to the renormalization are identified: the positive one given by the quartic anharmonicity and the negative one determined by the square of cubic anharmonicity. The ILM appears above the phonon spectrum when the first contribution exceeds the second one. For the monatomic chain with nearest neighbor interactions this condition agrees with that found by Kosevich and Kovalev [5] and it corresponds to a rather high ratio of quartic to cubic anharmonicities but in 3D lattices a smaller ratio is required. Our calculations demonstrate that in Ni and Nb this ILM condition is fulfilled. The molecular dynamics simulations for nickel and for niobium confirming this result are described in Section 3 followed by some conclusions in Section 4.

## II. THRESHOLD CONDITION FOR ILM

One can readily present an argument in favor of the localized mode possibility in metals. The point is that the essential contribution to the screening of the atomic interactions in metals comes from free electrons at the Fermi surface. Due to their well-defined energy and the oscillating character of the wave functions of these electrons

(Friedel oscillations) the resulting pair-potentials may acquire non-monotonic, or even oscillatory dependence on the atomic distance [26]. One consequence is that the ion-ion attractive force, at intermediate distances, may be enhanced resulting in an amplification of even anharmonicities for the resulting two-body potentials. This effect can counteract the underlying softening associated with the bare potentials with moderate increase of vibrational amplitudes to permit the existence of ILMs above the top of the phonon spectrum.

Let the anharmonic potential describing the nearest neighbor interactions for a 1-D monatomic chain be represented by

$$U = \sum_n \sum_{p=2}^4 \frac{K_p}{p} (u_{n+1} - u_n)^p \quad (1)$$

where  $K_2$  is the harmonic force constant and  $K_3, K_4$  are the anharmonic ones,  $u_n$  is the displacement of the  $n$ -th atom from its equilibrium position. The condition for the formation of an ILM with the frequency above the top of the phonon spectrum, given in Ref. [5], is  $\kappa = 3K_2K_4/4K_3^2 > 1$ .

To obtain the minimal condition more generally we use the equation for renormalization of the elastic springs of the atomic bonds by the ILM derived in Refs. [27, 28], which is

$$\delta K_{2n} = 2 \langle \sin^2(\omega_L t) \partial^2 V^{anh} / \partial r_n^2 \rangle, \quad (2)$$

where  $\delta K_{2n}$  is the change produced in the harmonic spring of the pair potential of bond number  $n$ . Here  $\omega_L$  is the frequency of ILM,  $V^{anh}$  is the anharmonic part of the potential, the second derivative is taken for the distance of the bond  $r_n = r_{0n} + \bar{A}_n \cos(\omega_L t) + \bar{\xi}_n$ , where  $r_{0n}$  is the length of the bond,  $\bar{A}_n$  is the amplitude of vibration of this bond,

$$\bar{\xi}_n = \sum_{n_l} \bar{g}_{nn_l} \langle \partial V^{anh} / \partial r_{n_l} \rangle \quad (3)$$

is the dc change (usually extension) of its length due to the ILM,  $\bar{g}_{nn_l} = g_{nn_l} - g_{n'n_l} - g_{nn_l'} + g_{n'n_l'}$ ,  $n$  and  $n'$  are the indexes of two ends of the bond  $n$ ,  $g_{nn_l} = -(M_n M_{n_l})^{-1/2} \sum_i e_{ni} e_{n_l i} \omega_i^{-2}$  is the static limit of the lattice Green's function,  $e_{ni}$  is the polarization vector of the phonon  $i$  for the bond  $n$ ,  $\omega_i$  is the frequency of the phonon,  $M_n$  is the mass of the atom  $n$ .

For a small amplitude ILM one need only consider cubic and quartic anharmonicity. In this approximation Eqs. (2) and (3) take the form

$$\delta K_{2n} = 2K_3 \bar{\xi}_n + \frac{3}{4} K_4 \bar{A}_n^2, \quad (4)$$

$$\bar{\xi}_n = \frac{1}{2} \sum_{n_l} \bar{g}_{nn_l} K_{3n_l} \bar{A}_{n_l}^2. \quad (5)$$

Usually the first term in Eq. (4) is negative while the second term is positive. The bond will harden with increasing amplitude of vibrations and an ILM will shift up from the phonon band if the absolute value of the first term is smaller than the second term. To fulfill this condition the value of the parameter  $\kappa$  needs to be sufficiently large. This value depends not only on the pair potentials but also on the type and dimension of the lattice.

We consider first  $\delta K_2$  in monatomic chain with nearest neighbor interactions. In this case  $n' = n + 1$  and  $g_{nn_l}$  depends on  $|n - n_l|$ . Therefore  $\bar{g}_{nn_l} = 2g_{nn_l} - g_{n+1n_l} - g_{n-1n_l}$ . From the equations of motion one gets  $\omega_i^2 e_{in} = (K_2/M)(2e_{in} - e_{in+1} - e_{in-1})$ . Multiplying both sides of this equation by  $\omega_i^{-2} e_{in_l}$  and summing up over  $i$  we get  $\delta_{nn_l} = -K_2 \bar{g}_{nn_l}$ . Consequently the dc lattice expansion equals

$$\bar{\xi} = -(K_3/2K_2) \bar{A}^2 \quad (6)$$

(index  $n$  is now omitted). Therefore

$$\delta K_2 = (3K_4/4 - K_3^2/K_2) \bar{A}^2. \quad (7)$$

The bond will harden with increasing amplitude of vibrations and an ILM will shift up from the phonon band if  $\kappa = 3K_2K_4/4K_3^2 > 1$ . This condition is identical to that found in Ref. [5] for localized vibrations in the chain. A detailed discussion of this condition also has been given in Ref. [29]. (For arbitrary amplitude the ILM condition for the potential described by Eq. (1) is given also in Ref. [30].)

Let us apply now Eqs. (4) and (5) to 3-D lattices. We treat an even symmetry ILM in a monatomic fcc or bcc lattice with the main motion directed along the shortest bond. Note that the high-energy edge of the phonon DOS in both these lattices corresponds to the short-wavelength phonons. Therefore the initial ILM under consideration, shifting up from the phonon band, resembles a wave packet of the standing longitudinal plane waves; it has a large spatial extent.

We assume that the anharmonic interactions are well localized. This allows one to include in Eq. (5) only contributions of the shortest bonds in the  $xy$ -direction (fcc lattice) or in  $xyz$ -direction (bcc lattice). The factors  $\bar{g}_{nn_l}$  in this equation tend to zero with increasing  $|n - n_l|$ . Therefore if the ILM is close to the threshold limit then the corresponding amplitudes of vibrations of all these bonds at the contributing  $n_l$  sites in Eq. (5) are almost the same and so the dc distortion

$$\bar{\xi} \simeq -\frac{2K_3 \bar{A}^2}{MN} \sum_q \sum_{n=0}^{N-1} \frac{1 - \cos(qr_0)}{\omega_q^2} e^{iqr_0(n-N/2)}, \quad (8)$$

where  $Nr_0$  is the distance between the border atoms in the direction of the main vibration ( $r_0$  the equilibrium first-neighbor distance),  $\omega_q$  is the frequency of the longitudinal waves,  $q$  is the wave number acquiring the discrete values  $q = \pi k/r_0 N$  with  $k = -N/2, -N/2 +$

1, ...  $N/2 - 1$  ( $N$  is even). In the  $N \rightarrow \infty$  limit only the term  $k = 0$  contributes so

$$\bar{\xi} = - \left( K_3 / 2\tilde{K}_2 \right) \bar{A}^2, \quad (9)$$

where  $\tilde{K}_2 = Mv_l^2/r_0^2$  is the mean elastic spring in the bulk,  $v_l$  is the longitudinal velocity of sound. Comparing this equation for  $\bar{\xi}$  with Eq. (6) and considering that  $\tilde{K}_2$  is larger than  $K_2$  we conclude that the expansion by an ILM in a 3D lattice is hindered as compared to the chain, - a physically intuitive result. Inserting Eq. (9) for  $\bar{\xi}$  into Eq. (4) we get  $\delta K_2$ . The hardening of the bonds in 3D lattices takes place and an ILM shifts up from the phonon band if

$$\tilde{\kappa} = 3\tilde{K}_2 K_4 / 4K_3^2 > 1. \quad (10)$$

This condition is easier to fulfill than the 1D condition for  $\kappa > 1$ .

### III. MD SIMULATIONS

#### A. ILMs in nickel

The potential energy of Ni developed in Ref. [31] has the customary form for the embedded atom model [24, 25]

$$E_{tot} = \frac{1}{2} \sum_{nn'} V(r_{nn'}) + \sum_n F_n(\bar{\rho}_n), \quad (11)$$

where  $V(r_{nn'})$  is a pair potential as a function of the distance  $r_{nn'}$  between atoms  $n$  and  $n'$ ,  $F_n$  is the embedding energy of atom  $n$  as a function of the electron density  $\bar{\rho}_n = \sum_{n' \neq n} \rho(r_{nn'})$  induced at atom  $n$  by all other atoms in the system,  $\rho(r_{nn'})$  is the electron density at atom  $n$  due to atom  $n'$  as a function of the distance between them. The second term in Eq. (11) is volume dependent. Its contribution is essential for determining the equilibrium configuration of the lattice. Below we use the effective pair format in which this term has only quadratic and higher-order contributions with respect to the displacement of atoms from their equilibrium position in the lattice. For small displacements compared to the lattice constant this term is usually small. In Ni corresponding correction of the elastic springs is of the order of 1%, and the correction of the anharmonic forces is even smaller.

The pair potential  $V(r)$  of Ni found from the data placed on the website [32] using the cubic spline approximation is presented in Fig. 1. In the same figure the approximation by the fourth-order polynomial using the least-square method in the interval  $2.496 \text{ \AA} \pm 0.116 \text{ \AA}$  is also presented. This interval corresponds to the actual values of coordinates of the ILM with the frequency near the top of the phonon band (see Table I). In this approximation  $K_2 \approx 2.32 \text{ eV/\AA}^2$ ,  $K_3 \approx -11 \text{ eV/\AA}^3$ ,

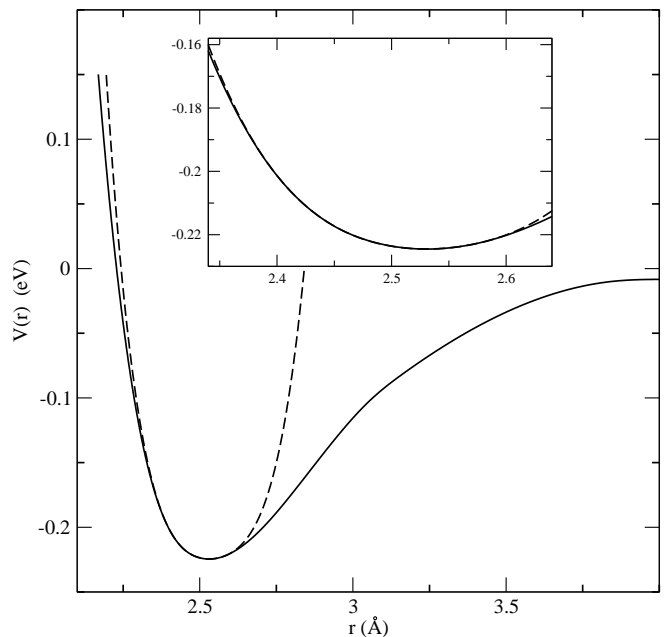


FIG. 1: The pair potential  $V(r)$  of Ni (solid line) and its approximation by the fourth-order polynomial (dashed line). Insert shows an expanded view.

$K_4 \approx 70 \text{ eV/\AA}^4$ . The root-mean-square deviation for the polynomial approximation in the given interval is  $10^{-5} \text{ eV}$ , i.e.  $\sim 1000$  times less than the corresponding vibrational energy of the bond.

The distance between the nearest atoms in Ni at room temperature  $r_0 = 2.49 \text{ \AA}$  and longitudinal sound velocity  $v_l = 5266 \text{ m/sec}$ . These values give  $\tilde{K}_2 = 2.75 \text{ eV/\AA}^2$ , (as expected  $\tilde{K}_2 > K_2$ ) and  $\tilde{\kappa} \approx 1.2$ . The distance  $r_0$  increases with temperature ( $r_0 = 2.51 \text{ \AA}$  at  $T = 800 \text{ K}$ ) while  $v_l$  decreases with temperature ( $v_l = 5100 \text{ m/sec}$  at  $T = 800 \text{ K}$ ). The  $\tilde{\kappa}$  value also decreases with temperature remaining at  $T = 800 \text{ K}$  somewhat larger than 1. Hence, in Ni the condition  $\tilde{\kappa} > 1$  is satisfied both at room and at high temperatures.

A fortunate circumstance is that the phonon DOS in Ni (and in other monatomic fcc lattices) has quite a sharp high frequency peak corresponding to the short-wave phonons (see Fig. 2) resulting in a straightforward localization of the wave packet of these phonons. Consequently one can expect that in Ni ILMs can exist with the frequency above the top of the phonon spectrum and that their amplitudes and hence corresponding energies may be relatively small.

To verify this prediction we performed MD simulations of vibrations of Ni clusters using the full two-body potential without polynomial approximation. Since the long-range interactions in metals are screened out the cluster calculations should give reliable results assuming that the size of the cluster is sufficiently large. In our calculations we studied clusters up to 22056 atoms with different boundary conditions: a) periodic, b) free ends,

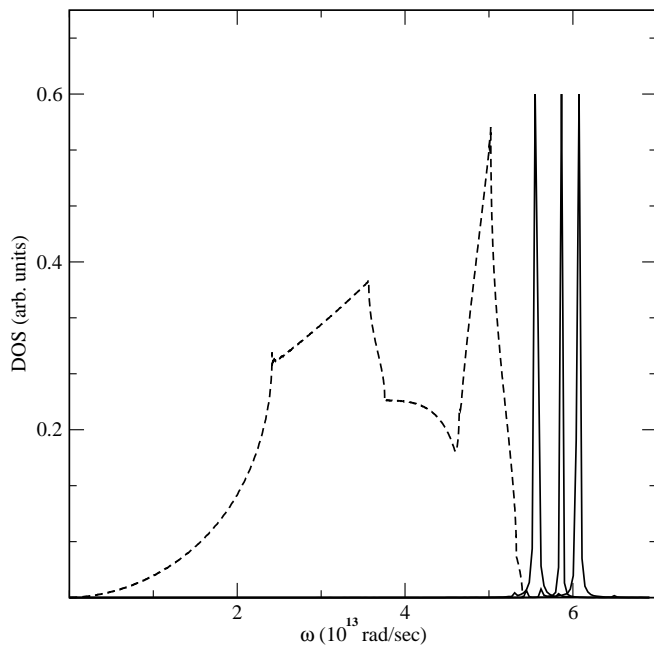


FIG. 2: Phonon density of states and three ILM spectral signatures for Ni. Phonon spectrum (dashed line) and spectrographs (solid line) of the different ILMs: The frequencies are 5.58, 5.86, 6.07 ( $10^{13}$  rad/sec) and the amplitudes of vibrations of the central bond are 0.18 Å, 0.31 Å and 0.42 Å.

c) fixed ends. The results of these calculations agree well with each other. Although the second (volume dependent) term in Eq. (11) gives only small corrections to forces, it was included in our MD simulations of clusters with periodic boundary conditions.

For the boundary conditions with free and fixed ends only the linear part of the second term in Eq. (11) was considered. We have found that this approximation does not noticeably change the results but allows one to significantly shorten the calculation time. The resulting phonon dispersion curves are in satisfactory agreement with those in the literature [31].

Classical molecular dynamics of a Ni cluster was calculated by means of the basic Verlet algorithm:

$$u(t + dt) = u(t) + v(t)dt + \frac{1}{2}a(t)dt^2, \quad (12)$$

$$v(t + dt) = v(t) + \frac{1}{2}(a(t) + a(t + dt))dt. \quad (13)$$

Here  $t$  is time,  $u(t)$  is displacement of the atom from its equilibrium position,  $v(t)$  and  $a(t)$  are the velocity and acceleration of the atom. The latter were found from Newton's second law by calculating the gradients of  $E_{tot}$  with respect to the atom coordinates. For the case of periodic boundary conditions the periodicity was a cube with edge 52.8 Å, which includes 13500 atoms. A time-step 2 fs was used; 7000 time steps have been calculated which corresponds approximately to 200 periods of vibrations of the ILM. The results of the calculations are given

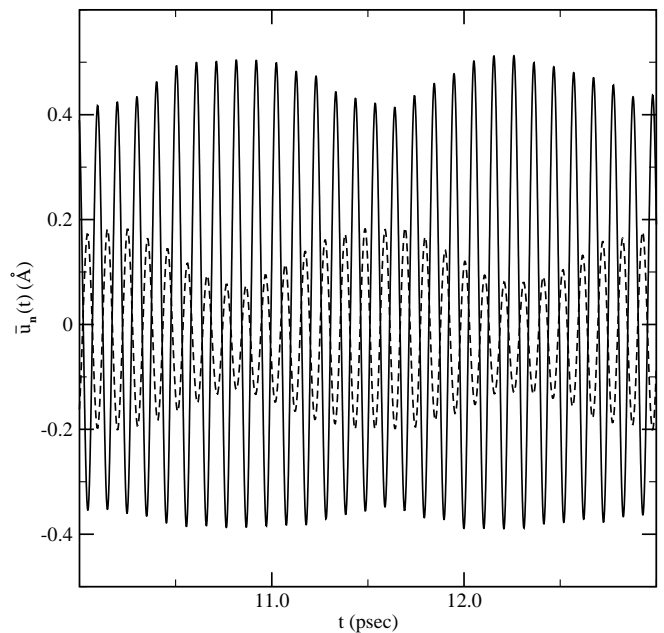


FIG. 3: Time dependence  $\bar{u}_n(t) = r_n(t) - r_0$  of the vibration of the central ( $n=0$ , solid line) and third ( $n=3$ , dashed line) bonds in Ni at long times containing the ILM with the frequency  $6.07 \cdot 10^{13}$  rad/sec. The corresponding values of the dc distortion  $\bar{\xi}_n$  are given in Table I. The amplitude modulation of the ILM is induced by its partner, the nearby linear local mode.

in Figs. 2 and 3 and in Table I. For the case of free ends the calculated cluster had 34 parallel  $40r_0 \times 17r_0$  square pallets; it includes 23120 atoms. A time-step of 0.01 fs was used. A few million time steps were calculated, so that the full calculated time would contain several hundreds of periods of ILM.

In the first runs to excite the lattice vibrations, 8 nearest central atoms located at  $\sqrt{2}r_0[n/2, n/2, 0]$ ,  $n = -4, -3, \dots, 3$  (in the central chain) have been initially displaced from their equilibrium position constituting an even structure; the displacements  $u_n$  of the atoms from their equilibrium position have been chosen as follows:  $u_0 = -u_1 = u_2 = -2u_3$ . This displacement pattern has the correct symmetry of the ILM but not the exact shape. The values of  $u_0$  varied from 0.09 Å to 0.3 Å. After the shake off of the phonons at short times the ILM was recognized as undamped periodic motion at large times (slowly modulated) at a frequency above the maximum of the phonon band. As an example of the corresponding time dependence of the vibration at long times, see Fig. 3, where the calculated dependence on time of the difference  $\bar{u}_n(t) = r_n(t) - r_0$  for two bonds  $n = 0$  and  $n = 3$  is given.

The dependence of the vibration frequency on amplitude of the central bonds is presented in Fig. 4; the vibrational amplitudes  $\bar{A}_n$  and the dc expansion  $\bar{\xi}_n$  of several bonds in the (110) direction are given on Table I. We also calculated several bonds in other directions;

the values of corresponding  $\bar{A}_n$  and  $\bar{\xi}_n$  appeared to be somewhat smaller. As follows from the Table I all seven ILMs presented are quite broad spatially, with the first three essentially keeping the same localization, and the other four ILMs broadening. Obviously this is a result of the softening of the pair potential as the amplitude of the ILMs increases. Still the amplitudes of all such ILMs decrease rapidly in the periphery as seen from the  $\bar{A}_6$  column.

To control the numerical procedure, the full energy of the cluster was calculated at every time step. The energy conservation law was found to be well fulfilled for the entire calculated time interval. We have also calculated the energy of the ILM; the contribution of 215

atoms situated in a prolate-ellipsoid shape was included in calculations. It appears that  $\sim 2/3$  of the energy of the initially displaced 8 central atoms remains localized, while again  $2/3$  of it belongs to the atoms in the initially excited chain and  $\sim 1/3$  goes to the nearest surrounding atoms. We have found that an ILM in Ni may have a rather small energy  $\sim 0.2$  eV (see the first line in the Table I). The reason is the existence of the narrow peak in the phonon DOS belonging to short-wave phonons, which permit a rapid splitting of the ILM away from the phonon band. On the other hand, for large  $\bar{A}_0 \geq 0.314$  Å one observes a significant difference between the ILM frequency and the top phonon frequency; thus we conclude that the existence of ILMs in Ni is reliable.

Table I. Spatial properties of ILMs in nickel. The difference of the frequency  $\omega_L$  of the even ILM and the maximum phonon frequency  $\omega_M = 5.4 \cdot 10^{13}$  rad/sec, amplitudes of the bonds  $\bar{A}_n$  and the changes of their length  $\bar{\xi}_n$  for the atoms located at  $\sqrt{2}r_0[n/2, n/2, 0]$ , with  $n = 0, 1, 2, 3, 6$ , and the resulting ILM energy  $E$ . The shifts of atoms of the central chain satisfy the condition  $u_{-n} = -u_{n-1}$ .

| $\omega_L - \omega_M$<br>( $10^{13}$ rad/sec ) | $\bar{A}_0$<br>(Å) | $\bar{A}_1/\bar{A}_0$ | $\bar{A}_2/\bar{A}_0$ | $\bar{A}_3/\bar{A}_0$ | $\bar{A}_6/\bar{A}_0$ | $\bar{\xi}_0$<br>(Å) | $\bar{\xi}_1/\bar{\xi}_0$ | $\bar{\xi}_2/\bar{\xi}_0$ | $\bar{\xi}_3/\bar{\xi}_0$ | $\bar{\xi}_6/\bar{\xi}_0$ | $E$<br>(eV) |
|--|--------------------|-----------------------|-----------------------|-----------------------|-----------------------|----------------------|---------------------------|---------------------------|---------------------------|---------------------------|-------------|
| 0.013  | 0.116              | 0.853                 | 0.534                 | 0.267                 | 0.050                 | 0.007                | 0.571                     | -0.143                    | -0.286                    | -0.0004                   | 0.204       |
| 0.081  | 0.142              | 0.845                 | 0.514                 | 0.239                 | 0.023                 | 0.008                | 0.750                     | -0.250                    | -0.375                    | -0.0005                   | 0.255       |
| 0.181  | 0.180              | 0.844                 | 0.522                 | 0.250                 | 0.034                 | 0.014                | 0.571                     | -0.143                    | -0.357                    | -0.0009                   | 0.366       |
| 0.465  | 0.314              | 0.863                 | 0.564                 | 0.287                 | 0.022                 | 0.034                | 0.618                     | -0.059                    | -0.235                    | -0.003                    | 1.080       |
| 0.672  | 0.420              | 0.905                 | 0.655                 | 0.365                 | 0.026                 | 0.048                | 0.729                     | 0.146                     | -0.354                    | -0.006                    | 2.197       |
| 0.742  | 0.474              | 0.945                 | 0.770                 | 0.508                 | 0.068                 | 0.040                | 0.975                     | 0.525                     | -0.175                    | -0.011                    | 3.474       |
| 0.779  | 0.500              | 0.966                 | 0.852                 | 0.640                 | 0.094                 | 0.030                | 1.100                     | 1.000                     | 0.267                     | -0.016                    | 4.596       |

## B. Slow modulation of ILM

Slow modulation of the ILM vibrational amplitude is observed in Fig. 3. The modulation is also seen as a satellite at the frequency  $\omega_{LL} = 5.6 \cdot 10^{13}$  rad/sec in the spectrum of vibrations of the bonds given in Fig. 5. The weak high-frequency satellite of the triple-peak in Fig. 5 results from the nonlinear four wave mixing  $2\omega_L - \omega_{LL}$ . This effect has been studied in some detail for a monatomic 1-D lattice in Ref. [33] and has been identified with linear local modes (LLMs) associated with the lattice perturbation produced by ILM.

To address the question whether the modulation observed for this 3-D system is connected with artificial size effects or LLMs we repeated the calculation for a cluster of twice larger size. No significant difference in the time dependence of vibrations of the central atoms have been observed. To perform an additional check on our interpretation of the origin of the modulation a second series of runs has been performed using as the initial conditions the long time displacement patterns of the 36 atoms (8 atoms in the central chain and 7 atoms in every nearest 4

chains) more closely registered to the correct ILM shape. Now the starting amplitudes of the central particles are determined by averaging over a modulation period. The time dependence of the vibration of the central ( $n=0$ ) and third ( $n=3$ ) bonds calculated in this way are presented in Fig. 6. Since the starting shapes more closely resemble a pure ILM eigenvector the only significant difference from the results shown in Fig. 3 is the reduction of the amplitude of modulation. The periods of the ILM vibration and of the modulation remain unchanged, precisely what is expected for an LLM of smaller amplitude. This removes the possibility that the observed modulation is associated with the reflection of phonon wave packets from the cluster boundary.

This conclusion also agrees with our calculation of vibrations of atoms near the border. The amplitudes of these border vibrations always remain less or of the order of  $5 \cdot 10^{-3}$  Å, i.e. they are much smaller than the amplitude of modulation of vibrations of the central atoms.

All of these signatures allow us to assign the observed modulation to the linear local mode produced by the ILM. Indeed, as expected for a LLM, its frequency increases with increasing amplitude and frequency of the

ILM. An enlargement of the modulation for the side bonds shows, in agreement with Ref. [33], that the maximum amplitude of the LLM is situated in the periphery of the ILM. An interesting property of the mode, which causes the modulation, is the change of the sign of the frequency difference  $\omega_L - \omega_{LL}$  with decreasing localization of the ILM. For the ILM in the first line of the Table I  $\omega_L - \omega_{LL}$  is negative ( $-0.14 \cdot 10^{13}$  rad/sec), while for ILMs in all other lines it is positive (0.17, 0.24, 0.42, 0.45, 0.38 and 0.35, respectively; all in  $10^{13}$  rad/sec units). This change of sign is also expected for the LLM: it results from the different dependence of the ILM and LLM on the even anharmonicities [33].

In order to verify the conclusion about the existence of ILMs in Ni at elevated temperatures we repeated the calculations presented in Fig. 6 for the lattice constant corresponding to 800 K. We have found that the ILM also exists at this temperature but with slightly enlarged ( $\sim 3\%$ ) amplitude and reduced frequency  $\omega_L = 5.67 \cdot 10^{13}$  rad/sec. Thermal fluctuations characteristic for non-zero temperature in the initial state have been ignored; however thermal-like fluctuations appeared in our MD simulations in the latter stages of the time-evolution of the system due to shaking-off of the phonons. These fluctuations do not significantly affect the ILM.

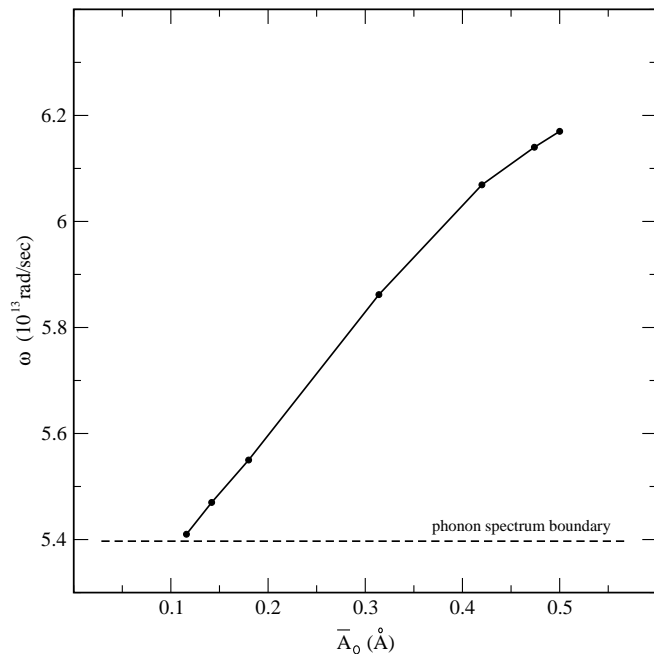


FIG. 4: The dependence of frequency  $\omega_L$  of the even ILM in Ni on the amplitude of vibrations of the central bond.

### C. ILMs in niobium

In contrast with nickel, niobium is isotopically pure and may provide a cleaner experimental signature for the

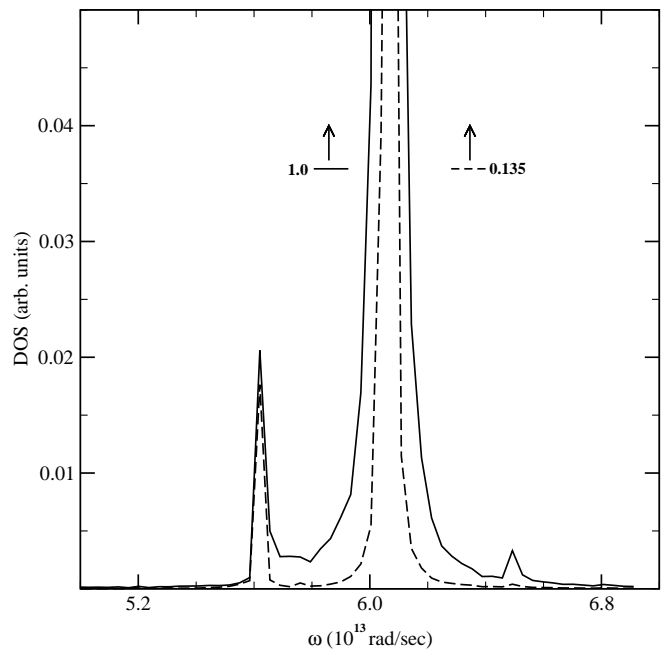


FIG. 5: ILM with its satellite LLM ( $\omega_L = 6.07 \cdot 10^{13}$  rad/sec). Shown are the Fourier transforms of vibrations  $\bar{u}_0(t)$  (solid line) and  $\bar{u}_3(t)$  (dashed line) given in Fig. 3.

observation of intrinsic localization. Using an analogous algorithm we also performed molecular dynamic simulations of ILMs in Nb. The peculiarity of this metal is the rather slow screening of the interactions with increasing distance between the ions. For a correct description of the phonon DOS one needs to take into account the elastic forces between at least six nearest neighboring atoms [34].

The existing EAM theories of Nb do not describe sufficiently well atomic forces for so large a spatial interval. Therefore we did not use them in a description of the linear dynamics. Instead, for this purpose the force constants for 6 nearest neighbors given in Ref. [34] were used. Thus, for Nb we did not use the single pair-potential for MD simulations (as we did it for Ni). Instead we used 6 different potentials (more precisely, we used 6 different forces) for every 6 nearest atom pairs.

The EAM potential of Ref. [35] was used only to find the anharmonic forces, namely, the 3 nonlinear forces for 3 nearest atoms. Corresponding to this EAM pair potential  $V(r)$  as well as its approximation by the fourth-order polynomial are presented in Fig. 7 (corresponding parameters equal  $K_2 \approx 1.5 \text{ eV}/\text{\AA}^2$ ,  $K_3 \approx -6.2 \text{ eV}/\text{\AA}^3$ ,  $K_4 \approx 65.6 \text{ eV}/\text{\AA}^4$ ; the root-mean-square deviation for the polynomial approximation in the interval between 2.82 and 2.97 Å is  $10^{-5}$  eV). This  $V(r)$  equals to the first term of EAM given by Eq. (3) in Ref. [35] plus the linear at  $r_0$  part of the second term in this equation ( $r_0$  is the equilibrium distance of the nearest atoms at given temperature). The anharmonic forces were found as follows: for each of 3 nearest atom pairs we deleted from the

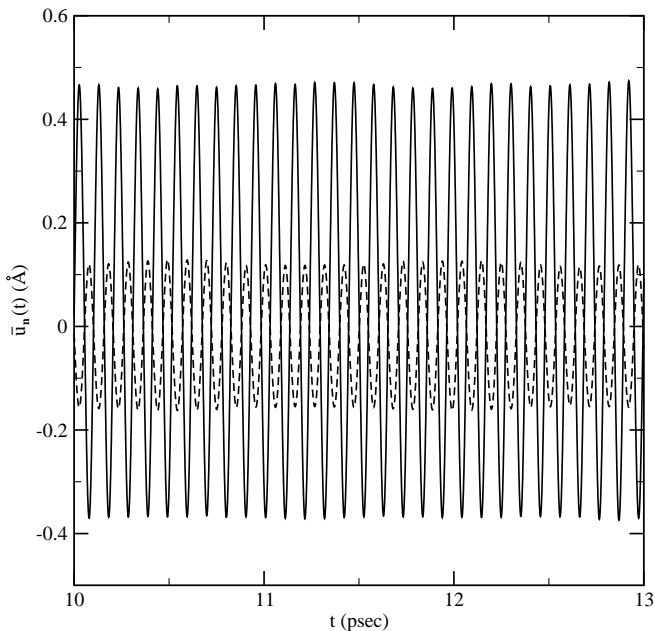


FIG. 6: The same time dependence  $\bar{u}_n(t) = r_n(t) - r_0$  of the vibration of the central ( $n=0$ , solid line) and third ( $n=3$ , dashed line) bonds in Ni at long times as shown in Fig. 3. The initial shifts of the 36 central atoms (8 atoms in the central chain and 7 atoms in every nearest 4 chains) more closely described by the correct ILM shape. The starting values of the shifts are obtained by averaging over a modulation period in Fig. 3. Since the ILM shape is more closely approximated the modulation amplitude is greatly reduced as compared to Fig. 3.

given in Fig. 7 potential the linear and quadratic terms at equilibrium distance. Then we added to each of these nonlinear forces the corresponding linear force given by Ref. [34].

The same source was used to obtain the remaining three linear forces between the atom pairs at larger distances. The justification for this approximation is that the relative change in distance of the fourth, fifth and sixth atom-pairs for the ILMs with the maximum amplitude  $\sim 0.1 \text{ \AA}$  is few percent. For such small relative shifts and large distances the anharmonic forces are negligibly small. Therefore for a description of ILMs with small amplitude, one may use the known elastic forces for six nearest neighbors [34] and to take into account the anharmonic forces only for three nearest neighbors.

Using the algorithm described above, we performed MD simulations of ILMs in Nb for room temperature 293 K (equilibrium first neighbor distance  $r_0=2.86 \text{ \AA}$ , longitudinal velocity of sound  $v_l=5380 \text{ m/sec}$ ) and high temperature 1773 K ( $r_0=2.89 \text{ \AA}$ ,  $v_l=5073 \text{ m/sec}$ ). For both temperatures  $\tilde{\kappa} > 1$ , i.e. the derived condition of an ILM with frequency above the phonon spectrum is fulfilled. The calculations at room temperature were made for a cluster containing  $2 \times 40 \times 40 \times 40$  moving atoms (altogether 128000 atoms). The calculations at high temperature were made for a cluster elongated in the [111]

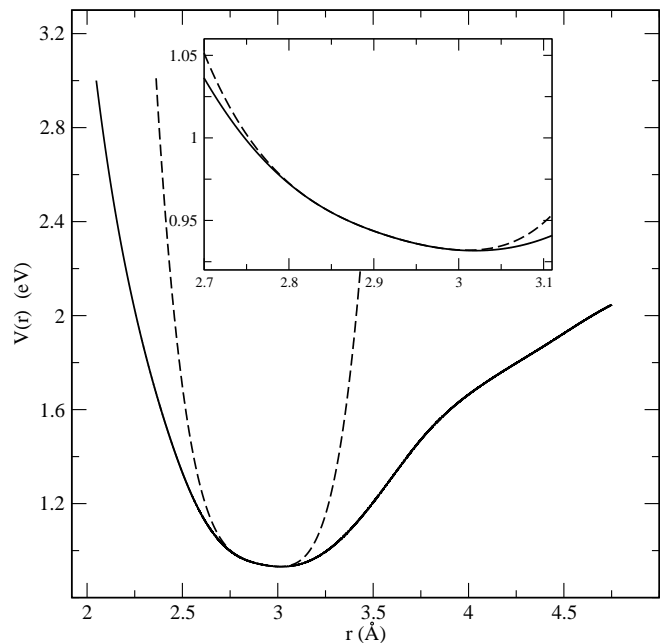


FIG. 7: The pair potential  $V(r)$  of Nb (solid line) and its approximation by the fourth-order polynomial (dashed line). Insert shows an expanded view.

direction with  $C_{3h}$  symmetry (a hexagonal prism) containing 18760 moving atoms. To minimize the calculation time, the positions and velocities of 1/6 of the atoms, situated in one of the six identical segments of the prism were calculated at every time step; the positions and velocities of all other atoms were found from the symmetry conditions.

For both sets of lattice parameters we have found even ILMs in the [111] direction of vibrations of the central atoms with frequencies above the top of the phonon spectrum. These ILMs are fully stable: no decay of their amplitude was observed over the last 500 periods of vibrations. A small periodic modulation of the amplitude, analogous to Ni was also observed, presumably caused by the appearance of a linear local mode. The spectra of ILMs for two different amplitudes of vibrations of the central bond are presented in Fig. 8 and 9 (together with the phonon spectrum). As expected the frequency of the ILM increases with amplitude.

To check the specificity of the above procedure we also performed calculations of ILMs in Nb taking into account the full potential given in Ref. [35] (including the volume-dependent second term in Eq. (10)). At high temperatures stable ILMs do exist for this model. In addition, we found that the formation of ILMs in Nb is favored by the expansion of the Nb lattice with increasing temperature.

On the other hand, based on the relations presented here, we have found that at least in some other metals (e.g. in Al and Cu) ILMs of the type described here should not exist. Indeed the values of the parameter  $\tilde{\kappa}$  in these metals at room temperature are found to be 0.3

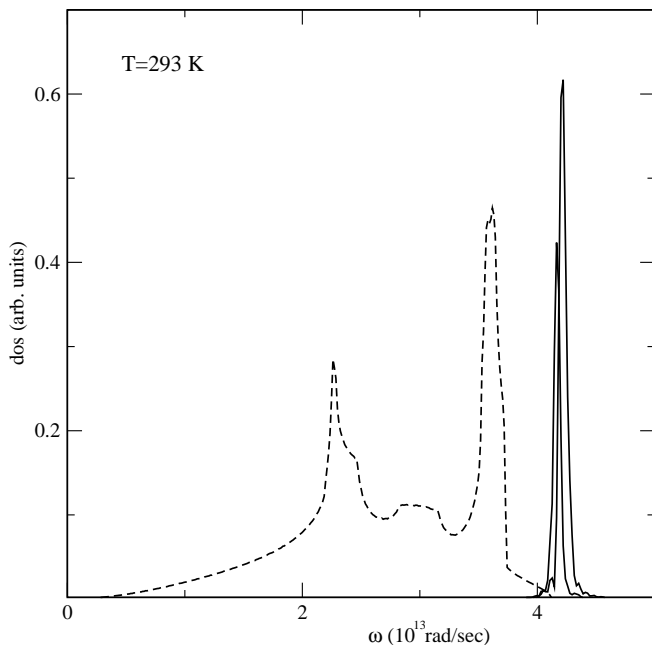


FIG. 8: Phonon DOS and spectra of even ILMs in Nb at room temperature 293 K for two amplitudes (0.25 Å and 0.3 Å) of vibrations of the central bond. Solid lines: ILMs, dashed line: phonon spectrum of Nb.

(Al) and 0.38 (Cu) (using the potentials given in Ref. [32]). At 800 K these parameters correspondingly equal 0.1 and 0.42. All these values are much smaller than the border value 1, which makes it unlikely that ILMs of the type described here can appear in these metals.

#### IV. CONCLUSION

To sum up we performed an analytic and numerical study of nonlinear dynamics of Ni and Nb and have found that intrinsic localized modes may exist in these metals with frequencies above the top of the phonon bands. The physical reason for this is the relatively large value of even anharmonicities as compared to odd ones produced by the free electron screening of the atomic interactions. As a result, in Ni and Nb (and, presumably in some other metals), the ion-ion attractive force, at intermediate distances is enhanced resulting in the amplification of even anharmonicities for the two-body potentials. This effect counteracts the underlying softening associated with the bare potentials with moderate increase of vibrational amplitudes to permit the existence of ILMs above the top of the phonon spectrum. In our MD simulations of nonlinear dynamics of Ni and Nb we have clearly observed ILM of this type. In addition we also observed the linear

local modes associated with an ILM; modes of this-type have been recently predicted and observed numerically for chains in Ref. [33]. According to our calculations an intrinsic localized mode in Ni or in Nb may have a rather

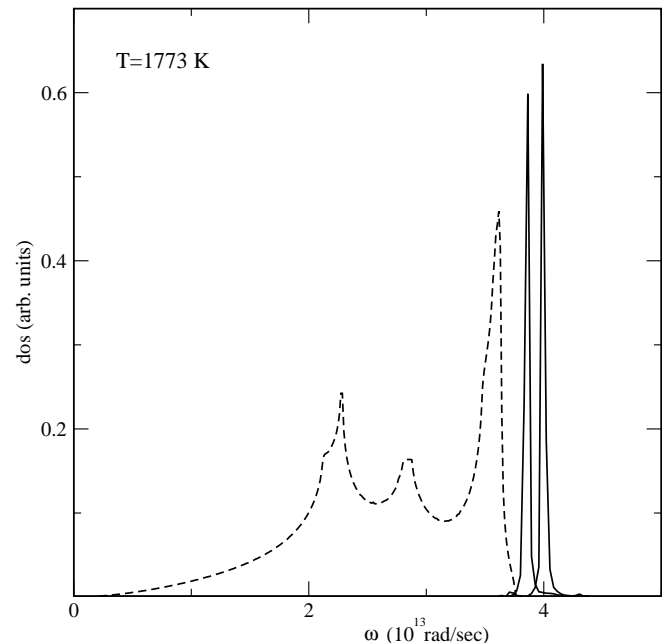


FIG. 9: Phonon DOS and spectra of even ILMs in Nb at a high temperature (1773 K) for two amplitudes (0.085 Å and 0.12 Å) of vibrations of the central bond. Solid lines: ILMs, dashed line: phonon spectrum of Nb.

small amplitude and hence a small energy of formation. We expect that in these metals ILMs may be observed as a high frequency features in the phonon spectrum at high temperatures. Finally we note that the precision of the existing EAM models of Nb is rather low [35, 36]; however, the EAM models of Ni are usually considered to be quite precise [31]. Therefore the conclusions presented here about ILMs in Ni are expected to be more reliable than those about ILMs in Nb.

#### V. ACKNOWLEDGMENTS

The research was supported by ETF grants no. 7741 and 7906 and by the European Union through the European Regional Development Fund (project TK114). AJS was supported by NSF-DMR-0906491.

[1] B. R. Henry, *J. Phys. Chem.* **80**, 2160 (1976).

[2] M. L. Sage and J. Jortner, *Adv. Chem. Phys.* **47**, 293

- (1981).
- [3] A. A. Ovchinnikov and N. S. Erihman, *Sov. Phys. Usp.* **25**, 738 (1982).
- [4] B. R. Henry and H. G. Kjaergaard, *Can. J. Chem.* **80**, 1635 (2002).
- [5] A. M. Kosevich and A. S. Kovalev, *Zh. Eksp. Teor. Fiz.* **67**, 1793 (1974) [*Sov. JETP* **40**, 891 (1974)].
- [6] A. S. Dolgov, *Fiz. Tverd. Tela (Leningrad)* **28**, 1641 (1986) [*Sov. Phys. Solid State* **28**, 907 (1986)].
- [7] A. J. Sievers and S. Takeno, *Phys. Rev. Lett.* **61**, 970 (1988).
- [8] J. B. Page, *Phys. Rev. B* **41**, 7835 (1990).
- [9] R. S. MacKay and S. Aubry, *Nonlinearity* **7**, 1623 (1994).
- [10] S. A. Kiselev and V. I. Rupasov, *Phys. Lett. A* **148**, 355 (1990).
- [11] S. R. Bickham, A. J. Sievers, and S. Takeno, *Phys. Rev. B* **45**, 10344 (1992).
- [12] K. W. Sandusky, J. B. Page, and K. E. Schmidt, *Phys. Rev. B* **46**, 6161 (1992).
- [13] A. J. Sievers and J. B. Page, in *Dynamical Properties of Solids: Phonon Physics The Cutting Edge*, edited by G.K. Norton and A.A. Maradudin (North Holland, Amsterdam, 1995), Vol. VII, p. 137.
- [14] S. Flach and C. R. Willis, *Phys. Repts.* **295**, 182 (1998).
- [15] R. Lai and A. J. Sievers, *Phys. Repts.* **314**, 147 (1999).
- [16] D. K. Campbell, S. Flach, and Y. S. Kivshar, *Physics Today* **57**(1), 43 (2004).
- [17] M. Sato, B. E. Hubbard, and A. J. Sievers, *Rev. Mod. Phys.* **78**, 137 (2006).
- [18] S. Flach and A. Gorbach, *Phys. Repts.* **467**, 1 (2008).
- [19] S. A. Kiselev, S. R. Bickham, and A. J. Sievers, *Phys. Rev. B* **48**, 13508 (1993).
- [20] S. A. Kiselev and A. J. Sievers, *Phys. Rev. B* **55**, 5755 (1997).
- [21] V. Hizhnyakov, D. Nevedrov, and A. J. Sievers, *Physics B* **316-317**, 132 (2002).
- [22] L. Z. Khadeeva and S. V. Dmitriev, *Phys. Rev. B* **81**, 214306 (2010).
- [23] M. E. Manley, M. Yethiraj, H. Sinn, H. M. Volz, A. Alatas, J. C. Lashley, W. L. Hults, G. H. Lander, and J. L. Smith, *Phys. Rev. Lett.* **96**, 125501 (2006).
- [24] M. S. Daw and M. I. Baskes, *Phys. Rev. B* **29**, 6443 (1984).
- [25] M. S. Daw and M. I. Baskes, *Phys. Rev. Lett.* **50**, 1285 (1983).
- [26] W. A. Harrison, *Solid State Theory* (McGraw Hill, New York, 1970).
- [27] V. Hizhnyakov, A. Shelkan, and M. Klopov, *Phys. Lett. A* **357**, 393 (2006).
- [28] A. Shelkan, V. Hizhnyakov, and M. Klopov, *Phys. Rev. B* **75**, 134304 (2007).
- [29] B. Sanchez-Rey, G. James, J. Cuevas, and J. F. R. Archilla, *Phys. Rev. B* **70**, 014301 (2004).
- [30] S. R. Bickham, S. A. Kiselev and A. J. Sievers, *Phys. Rev. B* **47**, 14206 (1993).
- [31] Y. Mishin, D. Farkas, M. J. Mehl, and D. A. Papaconstantopoulos, *Phys. Rev. B* **59**, 3393 (1999).
- [32] <http://cst-www.nrl.navy.mil/bind/eam>.
- [33] V. Hizhnyakov, A. Shelkan, M. Klopov, S. A. Kiselev, and A. J. Sievers, *Phys. Rev. B* **73**, 224302 (2006).
- [34] F. Guthoff, B. Hennion, C. Herzig, W. Petry, H. R. Schober, and J. Trampenau, *J. Phys. Cond. Mat.* **6**, 6211 (1994).
- [35] M. R. Fellingner, H. Park, and J. W. Wilkins, *Phys. Rev. B* **81**, 144119 (2010).
- [36] A. M. Guellil and J. B. Adams, *J. Mater. Res.* **7**, 639 (1992).